

AiCARR 50th International Congress; Beyond NZEB Buildings, 10-11 May 2017, Matera, Italy

## Indirect Evaporative cooling systems: modelling and performance analysis

Paolo Liberati<sup>a,\*</sup>, Stefano De Antonellis<sup>b</sup>, Calogero Leone<sup>a</sup>, Cesare Maria Joppolo<sup>b</sup>,  
Yakub Bawa<sup>a</sup>

<sup>a</sup>*Recuperator S.p.A., Rescaldina (MI), Italy*

<sup>b</sup>*Politecnico di Milano, Dipartimento di Energia, Milano (MI), Italy*

---

### Abstract

Nowadays, there are a lot of ongoing research activities about cooling technologies which can lead to a significant reduction in primary energy consumption of air handling units, in both residential and commercial applications. In this context, one of the most interesting technologies is the indirect evaporative cooling (IEC) system. In this work a phenomenological model of the component, based on a cross flow heat exchanger, has been developed and validated in typical summer operating conditions, at different air streams temperature, humidity ratio and flow rates. Using this tool, performance of the IEC system has been analyzed in different working conditions. Results highlight the advantage of using the IEC unit, which leads to significant energy savings in almost all the investigated conditions.

© 2017 The Authors. Published by Elsevier Ltd.

Peer-review under responsibility of the scientific committee of the AiCARR 50th International Congress; Beyond NZEB Buildings.

**Keywords:** indirect evaporative cooling, performance, cross flow, heat exchanger;

---

### 1. Introduction

The indirect evaporative cooling technology (IEC) is a solution that can be used in the air handling units to reduce the energy consumption during the summer period, both in residential and commercial applications.

---

\* Corresponding author. Tel.: +39 0331 1853 1.

E-mail address: [liberati@recuperator.eu](mailto:liberati@recuperator.eu)

In this system, the exhaust air, at ambient conditions, is humidified with water sprayed by the nozzles installed in proximity of the heat exchanger entrance; at the same time, the supply air, at outdoor temperature and humidity, is cooled down by the fresh and humid air of the opposite side.

Nowadays there are a lot of ongoing research activities about the IEC solutions; at the moment, main works have focused on studying prototypes [1, 7, 8] or particular operative conditions [5, 6]. Anyway there aren't works analyzing performance of IEC systems based on cross flow plate heat exchangers in typical summer conditions.

## Nomenclature

$A_{HE,net}$	Heat exchanger net cross section area, $m^2$
$cp$	Specific heat, $J\ kg^{-1}\ K^{-1}$
$C_w$	Wettability coefficient, -
$f_{eva}$	Fraction of the adsorbed water, -
$h$	Net channel height, m
$h_M$	Convective mass transfer coefficient, $kg\ s^{-1}\ m^{-2}$
$h_T$	Convective heat transfer coefficient, $W\ K^{-1}\ m^{-2}$
$k_W$	Plate conductivity, $W\ m^{-1}\ K^{-1}$
$L$	Net heat exchanger length, m
$\dot{m}$	Specific mass flow rate, $kg\ s^{-1}\ m^{-2}$
$N_{HE}$	Number of heat exchanger plates, -
$pt$	Heat exchanger plates pitch, m
$\dot{Q}$	Flow rate, $m^3\ h^{-1}$
$\dot{Q}_w$	Water flow rate sprayed on the heat exchanger, $l\ h^{-1}$
$T$	Temperature, $^{\circ}C$
$v$	Velocity, $m\ s^{-1}$
$x$	Primary air flow direction, m
$X$	Humidity ratio, $kg\ kg^{-1}$
$y$	Secondary air flow direction, m

## Greek symbols

$\delta$	Heat exchanger plates thickness, mm
$\Delta T$	Temperature difference, $^{\circ}C$
$\varepsilon$	Heat exchanger effectiveness, -
$\varepsilon_{wb}$	Wet bulb IEC effectiveness, -
$\rho$	Density, $kg\ m^{-3}$
$\sigma$	Wettability factor, -
$\varphi$	Relative humidity, -

## Subscript

$a$	Air
$ex$	Exhaust air
$HE$	Heat Exchanger
$in$	Inlet
$out$	Outlet
$su$	Supply air
$W$	Wall heat exchanger plates
$wb$	Wet bulb temperature

## Superscript

$N$	In reference conditions ( $\rho = 1,2\ kg\ m^{-3}$ )
-----	--

This research aims to fulfill this lack studying the IEC system in different operating conditions (namely air streams temperature, humidity ratio and flow rates). The work is divided into three parts. The first part deals with the description of the experimental setup and the test rig adopted in the research. The second part explains the developed model and its calibration process. The last part highlights the advantage of using the IEC unit through a parametric analysis based on the developed model. It is shown the indirect evaporative cooling technology leads to significant energy savings in all the investigated conditions, even with a low water flow rate.

## 2. IEC SYSTEM DESCRIPTION

A scheme of the analyzed indirect evaporative cooler is shown in Figure 1. The system consists of:

- A commercial cross-flow plate heat exchanger.
- N° 8 water spray nozzles.
- The equipment to increase pressure of water supplied to the nozzles.

The supply air stream is cooled in the heat exchanger at constant humidity ratio: it enters the system in condition  $su,in$  (assumed at outdoor air conditions) and it leaves the component in condition  $su,out$ . The exhaust air stream enters the system in condition  $ex,in$  (assumed at indoor air conditions - return air stream from the building) from the top plenum where water nozzles are installed. Due to the evaporation of water, the air stream is humidified almost at constant enthalpy from condition  $ex,in$  (before the plenum inlet) to condition  $ex,in,HE$  (at heat exchanger face). Finally, the secondary air stream leaves the system at condition  $ex,out$ . According to Figure 1 and to the actual experimental setup, the supply air stream crosses the heat exchanger from the right to the left and the exhaust air flow from the top to the bottom of the system.

Main data of the heat exchanger adopted in this study are summarized in Table I.

Table I. Main data of the investigated IEC system

Description	Parameter	Value
Number of plates	$N_{HE}$	119
Plate thickness	$\delta$	0.14 mm
Plate pitch	$pt$	3.35 mm
Net channel height	$h=pt-\delta$	3.21 mm
Net plate length and width	$L^*$	470 mm
Plate conductivity	$k_w$	220 W m <sup>-1</sup> K <sup>-1</sup>

Water nozzles are installed on two parallel manifolds (n° 4 nozzles on each one). The distance between each nozzle is around 8 cm and the two manifolds are installed at 15 cm from the heat exchanger face. According to data provided by manufacturer, the nominal water flow rate of each axial flow - full cone nozzle is 7.50 l h<sup>-1</sup> at 9 bar. Nozzles are installed in order to provide water in counter current arrangement respect to the secondary air stream. The length of top and side plenums is 42 cm and the length of bottom plenum is around 90 cm.

Inlet temperature, humidity ratio and flow rate of each stream are set through a dedicated air handling unit. Temperature and relative humidity are measured at the inlet and outlet of the investigated IEC system through RTD PT100 sensors ( $\pm 0.2^\circ\text{C}$  at  $20^\circ\text{C}$ ) coupled to capacitive relative humidity sensors ( $\pm 1\%$  between 0 and 90%). A detailed description of the experimental setup is available in previous works of the authors [2, 3].

## 3. IEC SYSTEM MODELING AND VALIDATION

The model of the indirect evaporative cooling system has been described and discussed in detail in a previous work of the authors [4]. Therefore, in this paper main assumptions and equations are briefly reported.

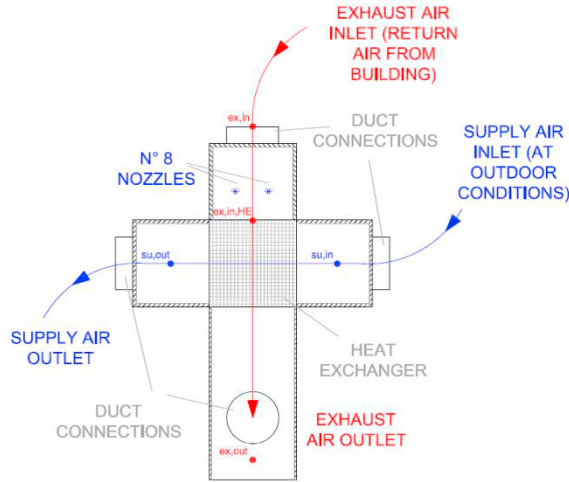


Fig. 1. Scheme of the experimental setup

Main adopted assumptions are:

- Steady-state conditions.
- No heat losses to the surroundings.
- Negligible axial heat conduction and water diffusion in the air streams.
- Negligible heat conduction in the heat exchanger plates.
- Uniform air inlet conditions.
- Interface plate temperature equal to bulk water temperature.

Referring to Fig. 2, energy and water mass balances have been applied to an infinitesimal element of the heat exchanger:

$$\frac{dT_{su}}{dx} = \frac{U_{T,su}(T_w - T_{su})}{v_{su}cp_{su}\rho_{su}\frac{h}{2}} \quad (1)$$

$$\frac{dT_{ex}}{dy} = \frac{h_{T,ex}(T_w - T_{ex})}{v_{ex}cp_{ex}\rho_{ex}\frac{h}{2}} + \frac{h_{M,ex}(\lambda + cp_{ex}T_{ex})(X_w - X_{ex})\sigma}{v_{ex}cp_{ex}\rho_{ex}\frac{h}{2}} \quad (2)$$

$$\frac{dX_{ex}}{dy} = \frac{h_{M,ex}(X_w - X_{ex})\sigma}{v_{ex}\rho_{ex}\frac{h}{2}} \quad (3)$$

$$h_{M,ex}(\lambda + cp_{ex}T_{ex})(X_{ex} - X_w)\sigma + h_{T,ex}(T_{ex} - T_w) + U_{T,su}(T_{su} - T_w) = 0 \quad (4)$$

$$\frac{d\dot{m}_w}{dy} = \frac{h_{M,ex}(X_{ex} - X_w)\sigma}{h/2} \quad (5)$$

Where  $\sigma$  is the fraction of wet surface area and  $U_{T,su} = 1/(1/h_{T,su} + \delta/kW)$ . The mass transfer coefficient is calculated assuming  $Le = 1$  as:

$$h_M = \frac{h_T}{cp_a} \quad (6)$$

According to the results reported in a previous work of the authors for the same heat exchanger [4], the heat transfer coefficient  $h_T$  is calculated through the following correlation:

$$h_T = \frac{k_a}{2h} 0.0185 \text{Re}^{0.928} \text{Pr}^{1/3} \quad (7)$$

Where  $k_a$  is the thermal conductivity of air and  $2h$  is the hydraulic diameter of the channel.

According to [4], the correlations to predict the saturation efficiency, the wettability factor and the coefficient  $C_w$  are respectively:

$$\varepsilon_h = \frac{c_1 \ln(T_{ex,in} - T_{ex,wb,in}) + c_2}{\dot{M}_s^{c_3}} \dot{M}_{w,in}^{c_4} \quad (8)$$

$$\sigma = \dot{m}_w \frac{h}{2 \delta_w v_w \rho_w} = \dot{m}_w C_w \quad (9)$$

$$C_w = \frac{k_1}{v_s^{N k_2} e^{k_3 \dot{m}_{w,in,HE}}} \quad (10)$$

Where  $\dot{m}_{w,in,HE} = \dot{m}_{w,in} - (X_{ex,in,HE} - X_{ex,in}) \dot{Q}_{exN} \rho_N / (3600 A_{HE,net})$  is the water specific mass flow rate, net of the water evaporation in the secondary air inlet plenum, and  $\dot{m}_{w,in} = \dot{M}_{w,in} / A_{HE,net}$ , with the net heat exchanger cross area  $A_{HE,net}$  equal to  $0.089 \text{ m}^2$ .

Due to the different plenum geometry adopted in this research, compared to the previous study of the authors [4], the parameters of Eqs. (8 – 10) have been fitted with experimental data (n° 30 tests), as summarized in Table 2. As a result it is:  $c_1 = -6.781$ ,  $c_2 = 33.97$ ,  $c_3 = 0.954$ ,  $c_4 = 0.984$ ,  $k_1 = 4.821$ ,  $k_2 = 0.0114$  and  $k_3 = 4.819$ .

In Fig. 3, the parity plot comparing experimental and numerical wet bulb effectiveness is reported for the data adopted in the calibration process (Table 2): in all cases the difference is within 3%. The effectiveness is defined as:

$$\varepsilon_{wb} = (T_{su,in} - T_{su,out}) / (T_{su,in} - T_{wb,ex,in}) \quad (11)$$

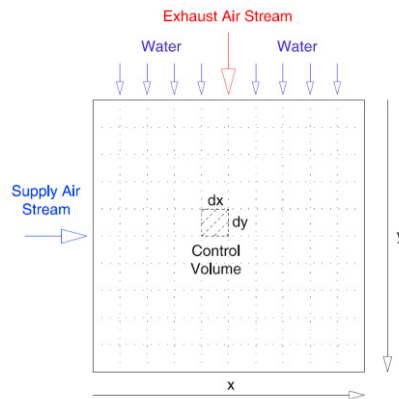


Fig. 2. Scheme of control volume adopted in the model

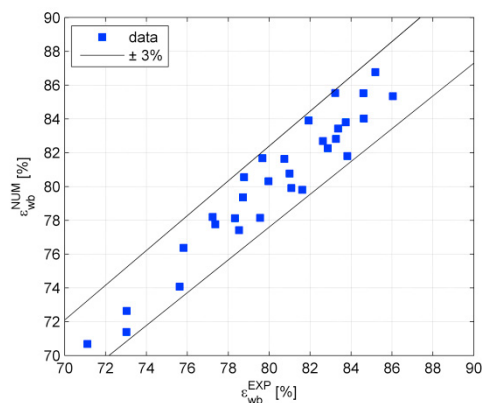


Fig. 3. Parity plot of wet bulb effectiveness (Data of Table 2)

Table 2. Main experimental data used for IEC model calibration

Test	$T_{ex,in}$ [°C]	$X_{ex,in}$ [g kg <sup>-1</sup> ]	$\dot{Q}_{ex}^N$ [m <sup>3</sup> h <sup>-1</sup> ]	$T_{su,in}$ [°C]	$X_{su,in}$ [g kg <sup>-1</sup> ]	$\dot{Q}_{su}^N$ [m <sup>3</sup> h <sup>-1</sup> ]	$\dot{Q}_{w,in}$ [l h <sup>-1</sup> ]
A	30.0	10.6	1200,1800	35.0	10.0	1200	30 - 60
B	30.0	13.4	1200,1800	35.0	10.0	1200	30 - 60
C	36.8	10.6	1200,1800	35.0	10.0	1200	30 - 60

#### 4. IEC performance: results discussion

In Fig. 4 to 6 the effect of different airflows, exhaust and supply air conditions and water flow rate on system performance is evaluated. The whole following analysis have been carried out considering the same plate heat exchanger and nozzles configuration described in section 2 and 3. Three conditions of water flow rate have been analyzed:

- no water flow (dry condition),
- $\dot{Q}_{w,in} = 15$  l/h.
- $\dot{Q}_{w,in} = 30$  l/h.

Three combinations of supply-exhaust airflow rate:

- $\dot{Q}_{su}^N = 1200$  m<sup>3</sup>/h and  $\dot{Q}_{ex}^N = 1200$  m<sup>3</sup>/h.
- $\dot{Q}_{su}^N = 1800$  m<sup>3</sup>/h and  $\dot{Q}_{ex}^N = 1800$  m<sup>3</sup>/h.
- $\dot{Q}_{su}^N = 1800$  m<sup>3</sup>/h and  $\dot{Q}_{ex}^N = 1200$  m<sup>3</sup>/h.

Comparison between experimental data has been performed through the following indexes: primary air temperature difference and fraction of evaporated water. Such quantities are defined in this form:

$$\Delta T_{su} = T_{su,in} - T_{su,out} \quad (12)$$

$$f_{eva} = \dot{Q}_{ex}^N \rho_a^N (X_{ex,out} - X_{ex,in}) / (\dot{M}_{w,in} 3600) \quad (13)$$

Results of the simulation with balanced airflow at 1200 m<sup>3</sup>/h are shown in Fig. 4: the water sprayed on the plate heat exchanger has a strong influence on the cooling capacity of the system; the higher is  $\dot{Q}_{w,in}$ , the higher is  $\Delta T_{su}$  in all the analyzed conditions. Compared to the dry condition (at  $T_{su,in} = 34^{\circ}\text{C}$ ), in case of water flow rate of 15 l/h the cooling capacity almost doubles; when  $\dot{Q}_{w,in} = 30$  l/h the cooling capacity increases around 120%. The evaporation of the water layer on heat exchanger plates, cools down the temperature of the plate surface and, consequently, increases significantly the system cooling capacity.

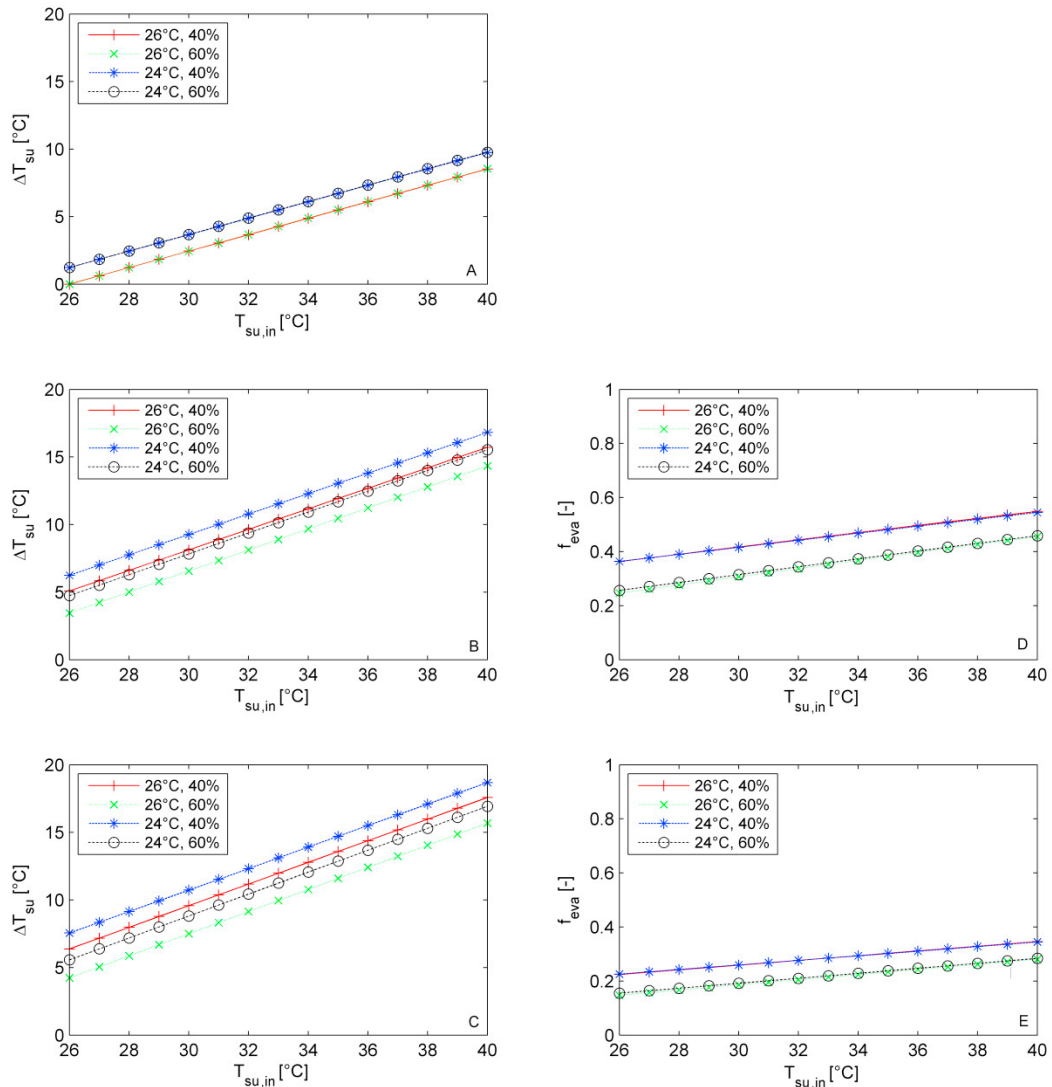


Fig. 4. Temperature difference between the inlet and outlet of the supply air flow in function of the outdoor temperature with  $\dot{Q}_{w,in} = 0$  l/h (A),  $\dot{Q}_{w,in} = 15$  l/h (B),  $\dot{Q}_{w,in} = 30$  l/h (C) and fraction of the evaporated water with  $\dot{Q}_{w,in} = 15$  l/h (D),  $\dot{Q}_{w,in} = 30$  l/h (E) for 4 different exhaust T and  $\phi$ .  $\dot{Q}_{su}^N = 1200$  m<sup>3</sup>/h  $\dot{Q}_{ex}^N = 1200$  m<sup>3</sup>/h

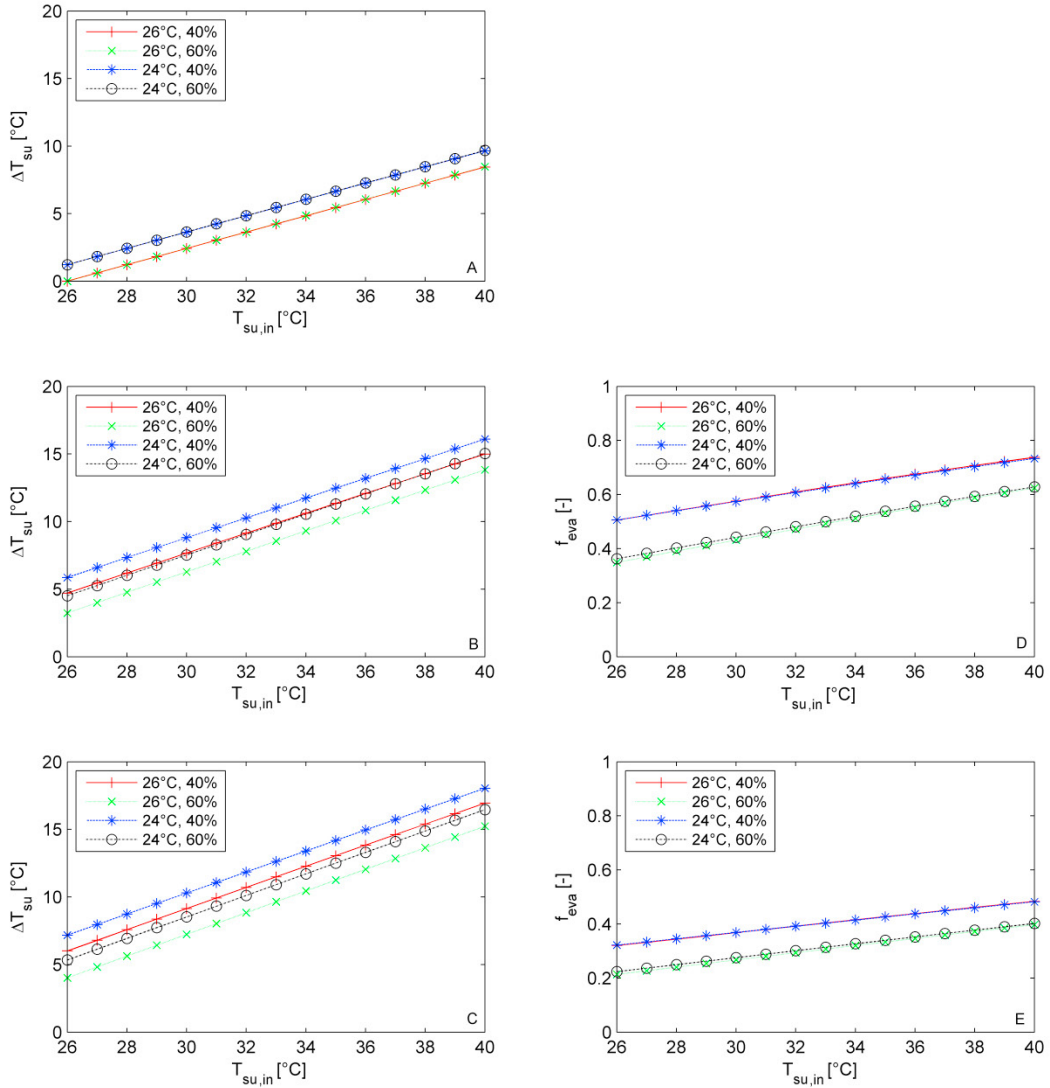


Fig. 5. Temperature difference between the inlet and outlet of the supply air flow in function of the outdoor temperature with  $\dot{Q}_{w,in} = 0$  l/h (A),  $\dot{Q}_{w,in} = 15$  l/h (B),  $\dot{Q}_{w,in} = 30$  l/h (C) and fraction of the evaporated water with  $\dot{Q}_{w,in} = 15$  l/h (D),  $\dot{Q}_{w,in} = 30$  l/h (E) for 4 different exhaust  $T$  and  $\phi$ .  $\dot{Q}_{su} = 1800$  m<sup>3</sup>/h  $\dot{Q}_{ex} = 1800$  m<sup>3</sup>/h

It should be noticed that the effect on the performance is greater in the range from  $\dot{Q}_{w,in} = 0$  to  $\dot{Q}_{w,in} = 15$  l/h than in the range from  $\dot{Q}_{w,in} = 15$  l/h to  $\dot{Q}_{w,in} = 30$  l/h. This is because the effect of the indirect evaporative cooling has an asymptotic behavior: at high water flow rates a high fraction of the heat exchanger surface is wet and the air stream reaches almost saturation conditions.

In the Fig. 4B different exhaust air conditions are compared. At constant outdoor temperature,  $\Delta T_{su}$  rises with the decreasing of relative humidity and temperature of the exhaust airflow: a lower dry bulb temperature of the exhaust air increases the sensible cooling capacity and a lower relative humidity promotes water evaporation. During the IEC process only part of water droplets evaporates in the exhaust air stream. The fraction of evaporated water



increases with the increase in  $T_{su,in}$  and the term  $T_{ex,in} - T_{wb,ex,in}$ . Quite obviously the  $\Delta T_{su}$  is higher for the condition  $T_{ex,in} = 24^\circ\text{C}$   $\phi_{ex,in} = 40\%$  than  $T_{ex,in} = 26^\circ\text{C}$   $\phi_{ex,in} = 40\%$  despite the fraction of the evaporated water is similar in both conditions. In the condition  $T_{ex,in} = 26^\circ\text{C}$   $\phi_{ex,in} = 40\%$  the fraction of the evaporated water varies from  $f_{eva} = 0.4$  to  $f_{eva} = 0.6$ . This value decreases with the increase of the water flow rate: when  $\dot{Q}_{w,in} = 30$  l/h the fraction of the evaporated water is always lower than  $f_{eva} = 0.4$ , even with high outdoor temperatures ( $T_{su,in}$ ).

In Fig. 5 it can be noticed the effect of the increase in the velocity of both supply and exhaust airflows. The increase in the airflow from  $\dot{Q}^N = 1200$  m<sup>3</sup>/h to  $\dot{Q}^N = 1800$  m<sup>3</sup>/h does not lead to a significant change in cooling performance both in dry condition (Fig. 5A) and in wet condition (Fig. 5B).

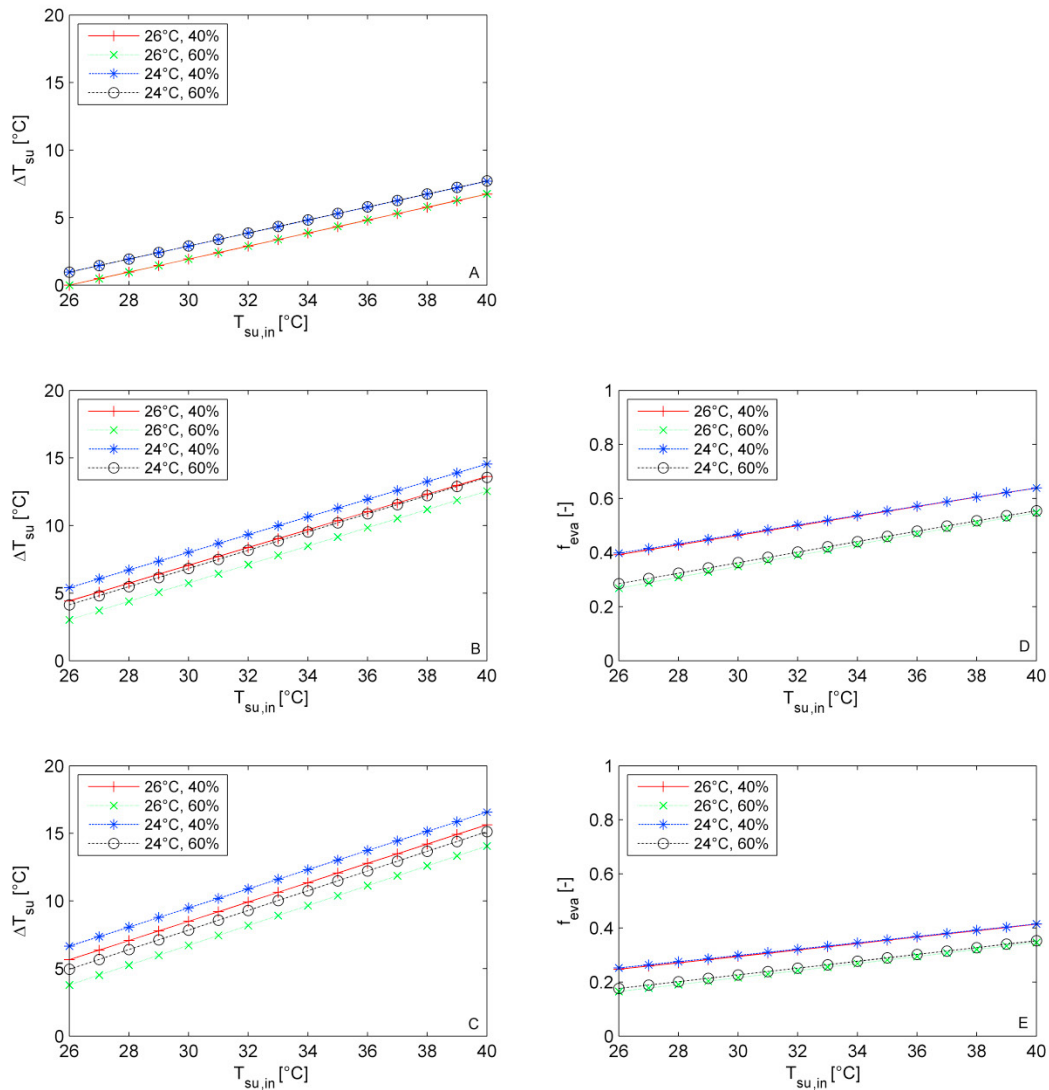


Fig. 6. Temperature difference between the inlet and outlet of the supply air flow in function of the outdoor temperature with  $\dot{Q}_{w,in} = 0$  l/h (A),  $\dot{Q}_{w,in} = 15$  l/h (B),  $\dot{Q}_{w,in} = 30$  l/h (C) and fraction of the evaporated water with  $\dot{Q}_{w,in} = 15$  l/h (D),  $\dot{Q}_{w,in} = 30$  l/h (E) for 4 different exhaust T and  $\phi$ .  $\dot{Q}_{su}^N = 1800$  m<sup>3</sup>/h  $\dot{Q}_{ex}^N = 1200$  m<sup>3</sup>/h

Comparing to Fig. 4, in dry condition only a slight decrease  $\Delta T_{su}$  occurs. In the wet condition, the increase in the airflow rate is partially compensated by the increase of the quantity of evaporated water; for instance, the fraction of the evaporated water reaches the value of 0.65 when  $T_{ex,in} = 26^\circ\text{C}$ ,  $\phi_{ex,in} = 40\%$  and  $T_{su,in} = 34^\circ\text{C}$  (Fig. 5D), which is 35% higher than in the condition reported in Fig. 4D.

In the AHU system the supply airflow rate is often higher than the exhaust air flow rate. The performance of the IEC system in condition with unbalanced flows is shown in Fig 6: the supply air is equal to  $\dot{Q}_{su}^N = 1800 \text{ m}^3/\text{h}$  while the exhaust air is  $\dot{Q}_{ex}^N = 1200 \text{ m}^3/\text{h}$ . In this condition  $\Delta T_{su}$  decreases around two degrees compared to results of Fig 4. On the contrary, the quantity of evaporated water, shown in Fig. 6D, is higher than the one of Fig. 4D because the average temperature of the plate is higher due to the higher supply air flow.

The quantity of supplied water on the system influences strongly the cooling capacity of the IEC (Fig. 7). At constant condition, with low water flow rate, the  $\Delta T_{su}$  rises steeply but it tends to an asymptotic value at high water flow rate. At a high water flow rate ( $\dot{Q}_{w,in} > 35 \text{ l/h}$ ), the cooling capacity slightly increases while the fraction of the evaporated water decreases consistently.

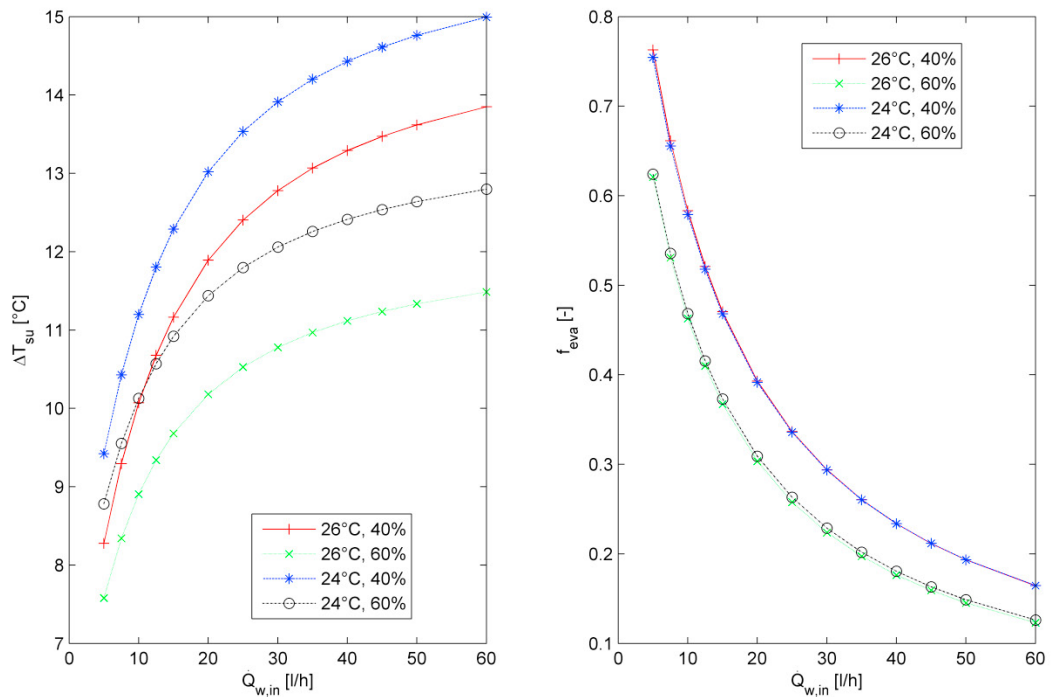


Fig. 7. Temperature difference between the inlet and outlet of the supply air flow in function of the water sprayed (A) and fraction of the evaporated water (B) for 4 different exhaust  $T$  and  $\phi$ .  $\dot{Q}_{su}^N = 1200 \text{ m}^3/\text{h}$   $\dot{Q}_{ex}^N = 1200 \text{ m}^3/\text{h}$ .  $T_{su,in} = 34^\circ\text{C}$

## 5. Conclusion

In this work, performance of an indirect evaporative cooling system has been discussed. A phenomenological IEC system model has been developed and calibrated with experimental data collected in a dedicated test facility.

With the model, the IEC system has been analyzed and significant results arose.

The water sprayed on the heat exchanger strongly increases the system cooling capacity even with very low flow rate: in the investigated conditions, when  $\dot{Q}_{w,in} = 15 \text{ l/h}$  the cooling capacity can be twice the one in dry conditions.

The fraction of the adsorbed water depends on the temperature and humidity condition of the two airflows, this value can rise up to  $f_{eva}=0.7$  with high supply and exhaust flow rate and low water flow rates.

Therefore, IEC systems can be an effective technology to achieve significant primary energy savings in HVAC operating in summer conditions.

## References

- [1] Bruno F. 2011. On-site experimental testing of a novel dew point evaporative cooler. *Energy and Buildings*, 43 (12), 3475-3483
- [2] De Antonellis S., Intini M., Joppolo C.M., Molinaroli L., Romano F. 2015. Desiccant wheels for air humidification: An experimental and numerical analysis. *Energy Conversion and Management*, 106, 355-364
- [3] De Antonellis S., Joppolo C.M., Liberati P., Milani S., Molinaroli L. 2016. Experimental analysis of a cross flow indirect evaporative cooling system. *Energy and Buildings*, 121, 130-138
- [4] De Antonellis S., Joppolo C.M., Liberati P., Milani S., Romano F. 2017. Modeling and experimental study of an indirect evaporative cooler. *Energy and Buildings*, 142, 147-157
- [5] Heidarinejad G., Bozorgmehr M., Delfani S., Esmaeelian J. 2009. Experimental investigation of two-stage indirect/direct evaporative cooling system in various climatic conditions. *Building and Environment* 44 (10) 2073-2079
- [6] Kim M.-H., Kim J.-H., Choi A.-S., Jeong J.-W. 2011. Experimental study on the heat exchange effectiveness of a dry coil indirect evaporation cooler under various operating conditions. *Energy*, 36 (11), 6479-6489
- [7] Saman W.Y., Alizadeh S. 2002. An experimental study of a cross-flow type plate heat exchanger for dehumidification/cooling. *Solar Energy*, 73 (1), 59-71
- [8] Tejero-González A., Andrés-Chicote M., Velasco-Gómez E., Rey-Martínez F.J. 2013. Influence of constructive parameters on the performance of two indirect evaporative cooler prototypes. *Applied Thermal Engineering*, 51 (1-2), 1017-1025
- [9] Zhang H., Shao S., Xu H., Zou H., Tian C. 2014. Free cooling of data centers: A review. *Renewable and Sustainable Energy Reviews*, 35, 171-182
- [10] Zhiyin D., Changhong Z., Xingxing Z., Mahmud M., Xudong Z., Behrang A., Ala H. 2012, Indirect evaporative cooling: Past, present and future potentials, *Renewable and Sustainable Energy Reviews* 16 (9) 6823-6850